



# Potential Utility of Synthetic D-Lactate Polymers in Skin Cancer

Anushka Dikshit<sup>1</sup>, Junqi Lu<sup>1</sup>, Amy E. Ford<sup>1</sup>, Simone Degan<sup>1</sup>, Yingai J. Jin<sup>1</sup>, Huiying Sun<sup>1</sup>, Amanda Nichols<sup>2</sup>, April K.S. Salama<sup>3</sup>, Georgia Beasley<sup>4</sup>, David Gooden<sup>5</sup> and Jennifer Y. Zhang<sup>1,6</sup>

Increased breakdown of glucose through glycolysis in both aerobic and anaerobic conditions is a hallmark feature of mammalian cancer and leads to increased production of L-lactate. The high-level lactate present within the tumor microenvironment is reused as a crucial biofuel to support rapid cancer cell proliferation, survival, and immune evasion. Inhibitors that target the glycolysis process are being developed for cancer therapy. In this study, we report an approach of using synthetic D-lactate dimers to inhibit melanoma and squamous cell carcinoma cell proliferation and survival. We also provide in vivo evidence that intratumoral injection of D-lactate dimers induced an innate immune response and inhibited subcutaneous melanoma xenograft growth in immunodeficient mice. Our findings support a potential utility of D-lactate dimers in skin cancer treatment and therefore warrant further mechanistic studies.

*JID Innovations* (2021);1:100043 doi:10.1016/j.xjidi.2021.100043

## INTRODUCTION

Enhanced glucose breakdown through glycolysis and consequently increased lactate production are hallmark features of mammalian cancer (de la Cruz-López et al., 2019; Feng et al., 2017; García-Cañaveras et al., 2019). The high-level lactate, up to 30–40 mM in the tumor microenvironment (TME) versus 1.5–3 mM in healthy tissues (Colegio et al., 2014), serves as a biofuel crucial for cancer cell proliferation and progression (Lu et al., 2015; San-Millán and Brooks, 2017). In addition, lactate enhances angiogenesis (Ruan and Kazlauskas, 2013) and inhibits innate and adaptive immune cell activities against cancer cells (Brand et al., 2016; Colegio et al., 2014; Feng et al., 2017; Fischer et al., 2007). Strategies that aim to block glycolysis using small-molecular inhibitors of glycolytic enzymes (e.g., Isonidamide and sodium dichloroacetate) and glucose analogs (e.g., 2-deoxy-glucose) have long been recognized as potential cancer therapeutics (Adeva et al., 2013; de la Cruz-López et al., 2019; García-Cañaveras et al., 2019). These strategies have shown promise, but their clinical benefit is often limited in part by the off-target effects and difficulties in

achieving high-dose delivery to tumor sites (Adeva et al., 2013; Feng et al., 2017; García-Cañaveras et al., 2019).

Human cells predominantly produce L-lactate, and L-lactate is precipitated by D-lactate polymers (Goldberg, 2011; Goldberg and Weinberg, 2018), stereoisomers commonly produced by the gut microbiome (Mayeur et al., 2013). It was previously reported that synthesized polymers of D-lactate formed stereocomplexes with L-lactate, leading to depletion of plasma level L-lactate. In addition, D-lactate dimers (DLADs) showed selective toxicity toward cervical and neuroblastoma cancer cells, sparing normal fibroblasts in culture (Goldberg, 2011). In this study, we examined the effects of DLADs on cultured melanoma and squamous cell carcinoma (SCC) cells, which are known to exhibit increased glycolysis (Houles et al., 2018; Ratnikov et al., 2017; Sun et al., 2010). We also examined the effects of DLADs on melanoma xenograft growth on immunodeficient mice.

## RESULTS

To assess effects on skin cancer, we first performed 3-(4,5-dimethylthiazol-2-yl)-2,5 diphenyl tetrazolium bromide–based cell growth analyses of melanoma cells. We found that DLAD inhibited the growth of A375 and A2058 human melanoma cells in a dose–response manner (Figure 1a). Next, we performed live and dead cell analysis by costaining with calcein-AM (Olympus BX41, Center Valley, PA) (green) and ethidium homodimer-1 (red), respectively. Microscopic images showed that 1-day treatment of 10 mg/ml DLAD resulted in complete cell death (Figure 1b). Consistently, DLAD inhibited mitochondria function in a dose–response manner, as shown by staining with the mitochondria activity–dependent red-fluorescent dye CMXRos (Figure 1c).

Next, we examined the in vivo effects of DLAD using subcutaneous melanoma xenografts generated with A2058 and A375 human melanoma cells in immunodeficient nude mice. When the tumors (n = 6–10 per group) reached a size of 166–200 mm<sup>3</sup>, we treated them by intratumoral injections

<sup>1</sup>Department of Dermatology, Duke University Medical Center, Durham, North Carolina, USA; <sup>2</sup>Department of Pediatrics, Duke University Medical Center, Durham, North Carolina, USA; <sup>3</sup>Department of Medicine, Duke University Medical Center, Durham, North Carolina, USA; <sup>4</sup>Department of Surgery, Duke University Medical Center, Durham, North Carolina, USA; <sup>5</sup>Department of Chemistry, Duke University, Durham, North Carolina, USA; and <sup>6</sup>Department of Pathology, Duke University Medical Center, Durham, North Carolina, USA

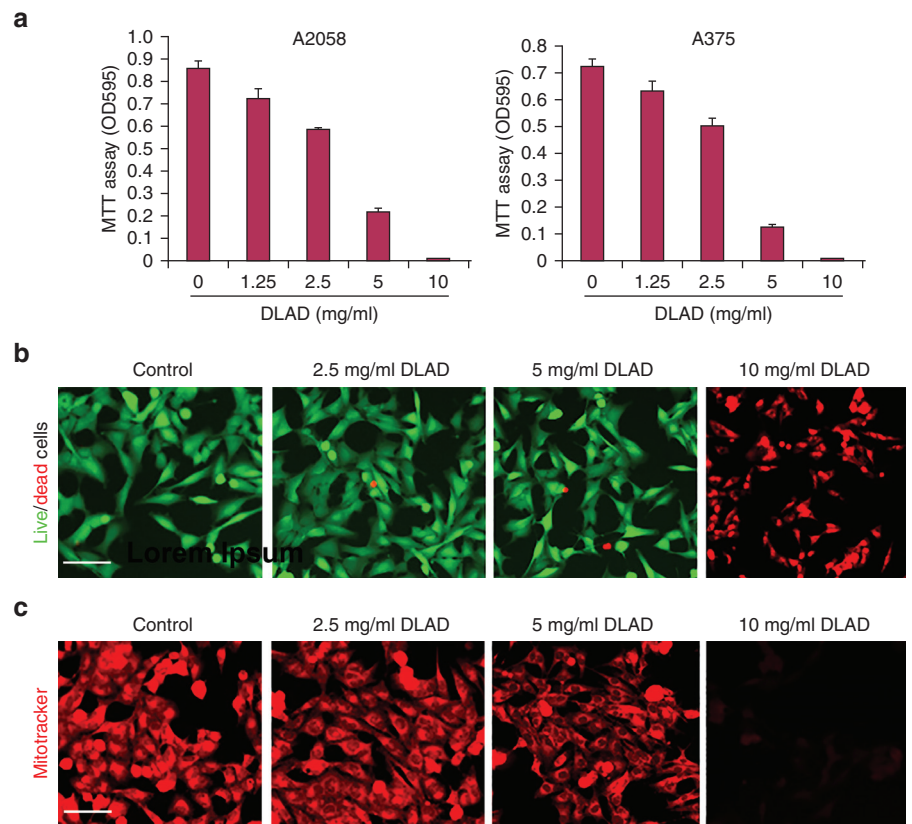
Correspondence: Jennifer Y. Zhang, Department of Dermatology, Duke University Medical Center, PO Box 103052, Durham, North Carolina 27710, USA. E-mail: Jennifer.zhang@duke.edu

Abbreviations: DLAD, D-lactate dimer; HEPES, 2-(4-[2-hydroxyethyl]piperazin-1-yl)ethanesulfonic acid; LLAD, L-lactate dimer; SCC, squamous cell carcinoma; TME, tumor microenvironment

Received 10 March 2021; revised 5 May 2021; accepted 1 June 2021; accepted manuscript published online 29 July 2021; corrected proof published online 28 August 2021

Cite this article as: *JID Innovations* 2021;1:100043

**Figure 1. DLAD inhibits melanoma cell proliferation and mitochondria function.** (a) MTT-based cell growth analysis. A2058 and A375 cells were treated with escalating doses of DLAD for 24 hours. Graphs represent the average optical reading  $\pm$  SD.  $P < 0.01$  was obtained between control and treated groups by Student *t*-test. (b) Live/dead cell analysis of A375 cells treated with DLAD for 24 hours by staining with calcein-AM (green)/ethidium homodimer-1 (red). (c) Mitochondria activity of A375 cells 24 hours after treatment with DLAD by staining with CMXRos. Images were taken under a Zeiss microscope. Bar = 50  $\mu$ m. DLAD, D-lactate dimer; MTT, 3-(4,5-dimethylthiazol-2-yl)-2,5-diphenyl tetrazolium bromide; OD, optical density.



of DLAD or PBS solvent control. We observed that tumors treated with DLAD showed an acute immune response within 24 hours after injection, and the inflamed areas resumed a normal skin appearance by the third week (Figure 2a). As expected, A375 and A2058 control tumors exhibited linear growth, reaching the end-point by the third week (Figure 2b and c). In contrast, those treated with DLAD at 25, 50, and 100 mg/ml doses were mostly regressed by the third week (Figure 2b and c).

L-lactic and D-lactic acids as well as their synthetic polymers are highly acidic ( $pK_a$  3.8). To assess whether DLAD effects were merely a result of acidity, we synthesized L-lactate dimers (LLADs), which are equally acidic as DLAD but do not form stereocomplexes with L-lactate (Goldberg, 2011). We found that although intratumoral injections of LLAD reduced tumor growth, the inhibition was significantly less effective than that of DLAD treatment (Figure 2c). By immunostaining, we found that DLAD-treated tissues were less proliferative than PBS- and LLAD-treated tissues, as indicated by the reduced number of Ki-67-positive cells (Figure 2d and e). These results indicate that DLAD treatment inhibits melanoma growth in vivo, and this biological effect is attributed to properties unique to DLAD and unlikely a mere result of acidity.

Consistent with the wounding response shown in Figure 2a, tumors treated with DLAD had increased infiltrations of F4/80<sup>+</sup> and CD45<sup>+</sup> innate immune cells, as shown by immunostaining (Figure 3). Thus, DLAD treatment inhibits melanoma growth and increases immune responses in vivo.

To further assess whether the biological activity of DLAD requires acidic pH, we used sodium phosphite dibasic to

control the pH. We found that DLAD after neutralization with sodium phosphite dibasic to pH 5.5 retained the growth inhibitory effects on A375 and A2058 melanoma cells when normalized to cells treated with equivalent concentrations of hydrochloric acid also adjusted with sodium phosphite dibasic to pH 5.5 (Figure 4a). Next, we examined whether DLAD has a potential utility in nonmelanoma skin cancers, which constitute the majority (>95%) of skin cancer. By 3-(4,5-dimethylthiazol-2-yl)-2,5-diphenyl tetrazolium bromide-based growth analysis, we found that DLAD showed dose-response effects on all SCC cell lines examined, including A431, Fadu, and CAL27. By 72 hours after treatment of DLAD at 3.75 mg/ml concentration, SCC cells were lifted with minimal metabolic activity, whereas fibroblasts remained attached and showed a flattened growth curve (Figure 4b). Finally, we explored various biologically suitable buffer systems and determined that compared with sodium phosphite dibasic ( $pK_a$  6.8–7.2), 2-(4-[2-hydroxyethyl]piperazin-1-yl)ethanesulfonic acid (HEPES) ( $pK_{a1}$  3 and  $pK_{a2}$  7.5) has high solubility and capacity in adjusting pH under changes in carbon dioxide concentrations during cell culture. We found that after adjustment to pH 6.2 with HEPES buffer, equivalent concentrations of hydrochloric acid-HEPES and DLAD-HEPES both slowed cell proliferation. However, DLAD-HEPES was more effective than hydrochloric acid-HEPES in inhibiting the proliferation of CAL27 cancer cells and displayed a substantially reduced toxicity to normal fibroblasts compared with that to SCC cells (Figure 4c). When neutralized to pH 7.0, both hydrochloric acid and DLAD were no longer toxic toward cancer cells and normal fibroblasts (Figure 4c).

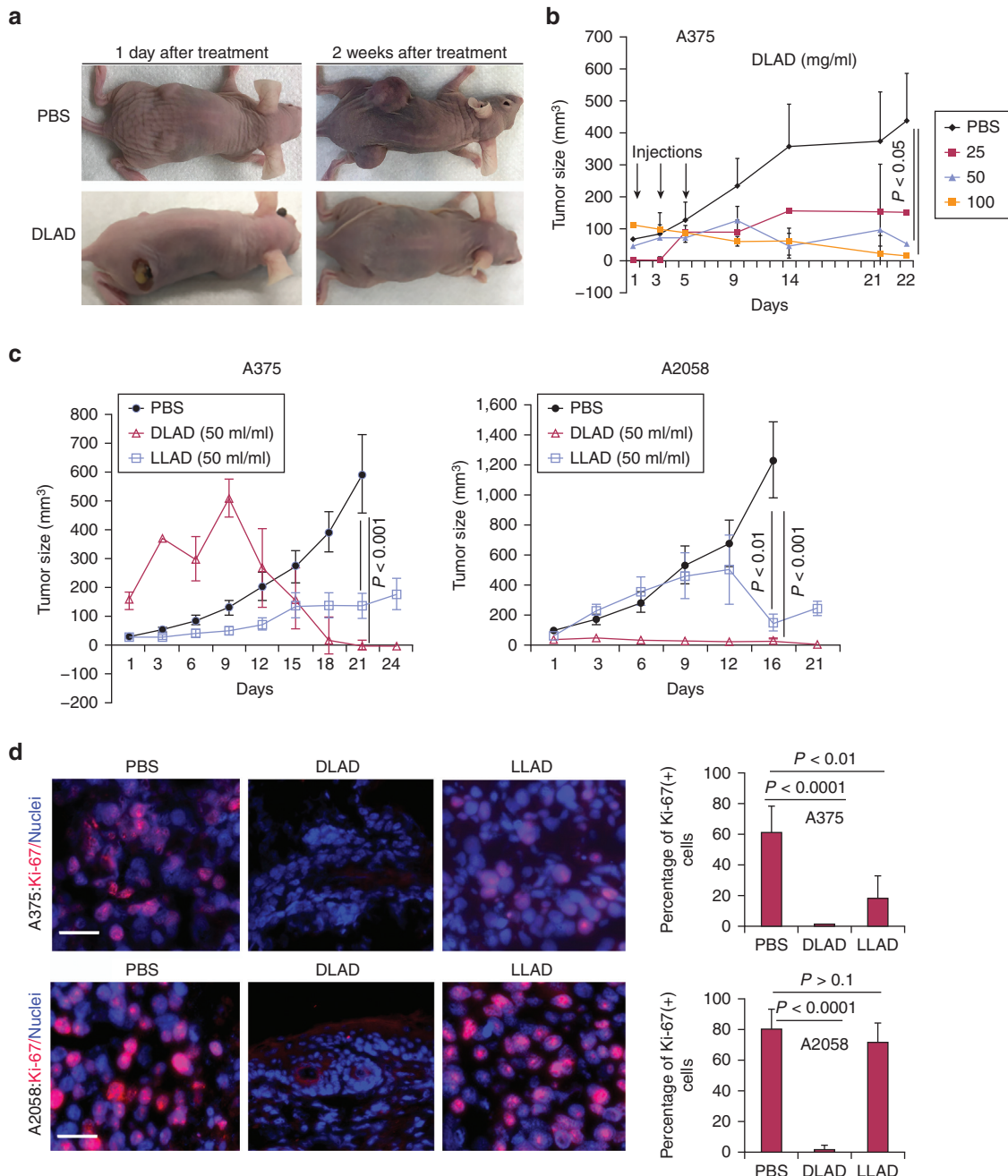


**Figure 2. DLAD inhibits melanoma growth in mice.** (a) Representative images were taken 1 day and 2 weeks after intrasplenic injection of PBS or DLAD (100 mg/ml). (b) Subcutaneous A375 melanoma growth on immunodeficient mice. Melanoma nodules (n = 5–6 per group) were treated with three intratumoral injections of PBS vehicle control or 25, 50, and 100 mg/ml DLAD delivered every other day. The graph depicts the average tumor size  $\pm$  SD. (c) Subcutaneous A375 and A2058 melanoma growth on immunodeficient mice. Subcutaneous melanoma (n = 6–10 per group) was treated with 3–5 injections of PBS, DLAD, or LLAD (50 mg/ml) every other day. The graph depicts the average tumor size  $\pm$  SD. Note that the measurements included wounded areas, which explains the initial growth of A375 tumors. (d) Immunostaining for Ki-67 (orange) and nuclei (blue). Graphs represent the average percent of Ki-67–positive cells. In total, 7–10 images per group were analyzed. Bar = 50  $\mu$ m. DLAD, D-lactate dimer; LLAD, L-lactate dimer.

These results indicate that DLAD is toxic to melanoma and nonmelanoma cancer cells and that an increased specificity of DLAD toxicity to cancer cells versus to normal cells may be achieved at a mildly acidic environment with a pH around 6.2.

In summary, we have identified DLAD as a potential treatment for skin cancer using in vitro and in vivo models of melanoma and SCC. Treatment with DLAD inhibited

melanoma growth and induced a robust activation of the innate immunity as evidenced by the acute wounding response and the increased infiltration of CD45<sup>+</sup> and F4/80<sup>+</sup> innate immune cells. These results warrant further investigation to understand the molecular mechanisms responsible for DLAD-induced killing of cancer cells as well as the effects of DLAD on the tumor vasculature and immune cells within and outside of the TME.

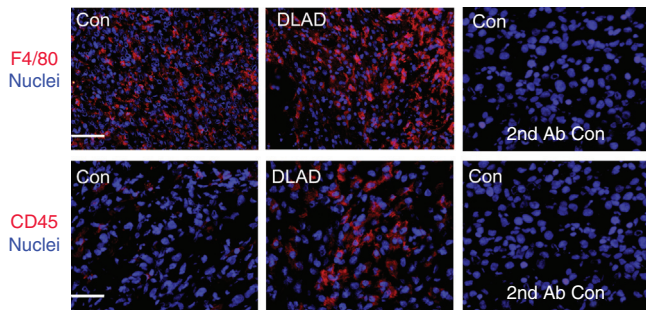


**Figure 3. DLAD induces immune cell infiltration.** Immunostaining of A2058 subcutaneous melanoma xenografts treated with PBS or DLAD (25 mg/ml) for F4/80 and CD45 (orange) and nuclei (blue). Bar = 100  $\mu$ m. Ab, antibody; Con, control; DLAD, D-lactate dimer.

## DISCUSSION

Although the mechanism of cancer cell killing remains unclear, one hypothesis is that DLAD sequesters extracellular L-lactate, preventing its uptake and utilization by cancer cells for rapid energy production and biosynthesis. However, it is possible that the DLAD may itself enter cancer cells and directly disrupt cellular metabolism. In addition, DLAD may interfere with the cellular metabolism of noncancer cells within the TME that support cancer cell proliferation and survival. These include the tumor vasculature and the innate and adaptive immune cells that rely on L-lactate for angiogenesis (Ruan and Kazlauskas, 2013) and immune inactivity toward cancer cells (Brand et al., 2016; Colegio et al., 2014; Feng et al., 2017; Fischer et al., 2007), respectively. Again, DLAD effects on TME cells may be linked to the depletion of extracellular L-lactate and direct uptake by TME cells, leading to disruption of metabolic pathways.

The *in vitro* data showed that the biological effects of DLAD require an acidic condition ( $\text{pH} < 7.0$ ). In this regard, TME ( $\text{pH} 6.7\text{--}7.1$ ) is generally more acidic than differentiated normal tissues ( $\text{pH} 7.4$ ), and acidosis of TME is commonly considered tumorigenic and important for tumor invasion, metastasis, immune evasion, and neoangiogenesis (Tannock and Rotin, 1989; Webb et al., 2011). On one hand, extracellular acidosis ( $\text{pH} \leq 6.7$ ) is found to trigger human melanoma cell senescence (Böhme and Bosserhoff, 2020). DLAD has a  $\text{pK}_a < 4$ , and intralesional administration of DLAD likely decreases TME extracellular  $\text{pH}$  to well below 6.7 and therefore induces senescence. Contrary to the acidic environment of TME, the intracellular  $\text{pH}$  of cancer cells is generally more alkaline ( $\text{pH} > 7.2$ ) than that of normal cells ( $\text{pH} 7.2$ ), and this characteristic is crucial for cancer cell proliferation and survival (Webb et al., 2011). This reversed  $\text{pH}$  gradient of extracellular acidosis and intracellular alkalization represents a cancer cell hallmark and is hence recognized as a potential target for cancer therapy (Persi et al., 2018; Webb et al., 2011). Potential entrance of DLAD into cancer cells will lead to acidification of the intracellular space and may therefore represent another mechanism of cancer cell killing.

Systemic acidosis is detrimental to human health. Thus, we anticipate that DLAD is not suitable for systemic treatment. In contrast, despite local toxicity, systemic toxicity was not apparent in mice that received multiple intralesional

injections of DLAD, implicating that intralesional delivery of a similar quantity of DLAD to cubic centimeter size tumors will unlikely induce systemic adversity in the human body. Synthetic lactate oligomers are biodegradable and have been widely used in medical products and dermal fillers (Liu et al., 2019), further supporting the feasibility of DLAD for cancer treatment.

It was recently reported that gut microbiomes modulate the outcome of melanoma response to PD-1 inhibitor immunotherapy. Specifically, commensal bacteria enriched in the anabolic pathways are associated with a favorable outcome for patients with melanoma (Gopalakrishnan et al., 2018; Matson et al., 2018). An emerging question is whether gut microbiomes act through common metabolites such as lactate to modulate cancer immune responses and whether DLAD has beneficial effects on this process. Understanding the effects of DLAD on local and systemic adaptive immunity will ascertain the utility of DLAD as a local adjuvant therapy that enhances systemic therapies such as PD-1/PD-L1 and CTLA-4 immune checkpoint inhibitor therapies as well as BRAF/MAPK/extracellular signal-regulated kinase kinase oncokine inhibitors and oncolytic therapies (Bai and Flaherty, 2020).

Skin cancer is the most common form of human cancer, and the incidence and the economic burden for treating melanoma and nonmelanoma skin cancer are skyrocketing (Guy et al., 2015a; Rogers et al., 2015) (<https://www.cancer.org/cancer/skin-cancer.html>). In 2011, the cost for skin cancer treatment was around \$8.1 billion (\$4.8 for non-melanoma skin cancer and \$3.3 billion for melanoma) in the United States (Guy et al., 2015b) and is expected to increase substantially by 2030 (Guy et al., 2015b). The most common treatments for primary skin cancer are tumor destruction with electrodesiccation and curettage, cryosurgery, simple excision, and Mohs surgery (Chren et al., 2013). The use of biological agents has increased over the recent years. Among these are 5-fluorouracil, imiquimod, ingenol mebutate, and retinoid (Cullen et al., 2020) as well as small-molecule inhibitors of the Shh pathway (Tang et al., 2011) and immune checkpoint inhibitors such as cemiplimab (Migden et al., 2018). Topical and intralesional treatments allow for higher drug levels at the tumor site than systemic agents (Cullen et al., 2020), alleviating systemic toxicity and potentially reducing overall cost. It is conceivable that with additional studies, DLAD may offer a new treatment option for skin cancer.

## MATERIALS AND METHODS

### Cell culture and reagents

A375, A2058, A431, CAL27, and Fadu cells were obtained from ATCC (Manassas, VA) through Duke Cell Culture Facility (Durham, NC). Primary fibroblasts were isolated from surgically discarded foreskin samples obtained by an exempt Institutional Review Board protocol approved by the Duke University (Durham, NC). Patient consent for experiments was not required because the United States laws consider human tissue left over from surgery as discarded material. All cells were cultured and maintained in DMEM with 10% fetal bovine serum and  $\times 1$  antibiotic/antimycotic (100 units/ml of penicillin, 100  $\mu$ g/ml of streptomycin, and 0.25  $\mu$ g/ml of Gibco

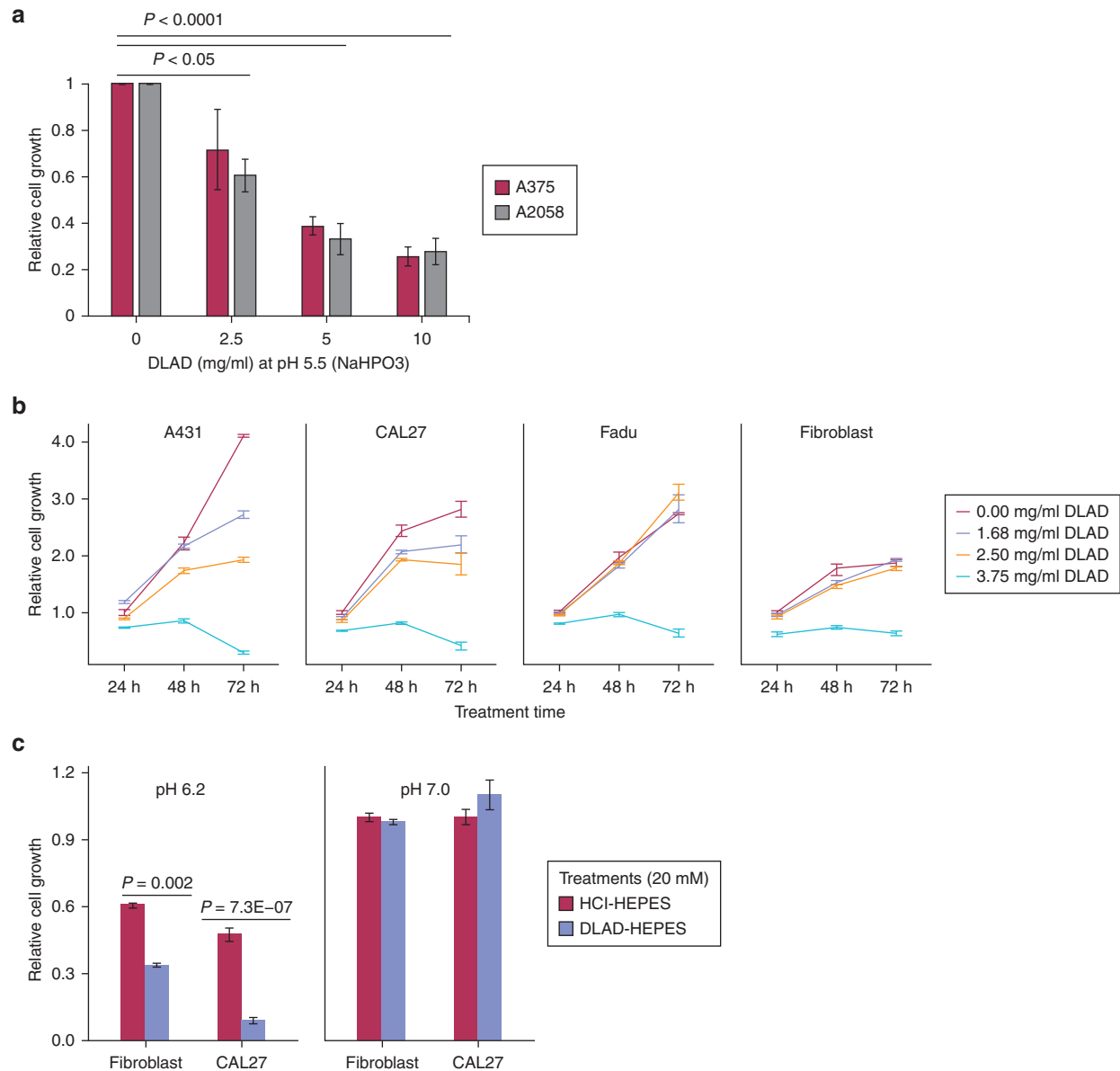


**Figure 4. DLAD retains toxicity to cancer cells at pH 6.2.** (a) MTT cell growth analysis. A375 melanoma cells were treated with increasing concentrations (2.5, 5, 10 mg/ml) of Na<sub>2</sub>PO<sub>4</sub>-neutralized DLAD or LLAD for 24 h. Graphs represent the average optical reading (OD595) ± SD. (b) MTT-based cell growth analysis of A431, CAL27, and Fadu cancer cells as well as normal dermal fibroblasts treated with escalating doses of DLAD for 24, 48, and 72 h. (c) MTT-based cell growth analysis of CAL27 cancer cells and normal dermal fibroblasts treated with 20 mM DLAD for 72 h. DLAD (20 mM) was neutralized with HEPES buffer to pH 6.2 and pH 7. Sodium chloride and HCl were used for controls. The graph represents the averages of relative cell growth normalized to respective controls at pH 7 ± SD. *P*-values were obtained by two-tailed Student's *t*-test. DLAD, D-lactate dimer; h, hour; HCl, hydrochloric acid; HEPES, 2-(4-[2-hydroxyethyl]piperazin-1-yl) ethanesulfonic acid; LLAD, L-lactate dimer; MTT, 3-(4,5-dimethylthiazol-2-yl)-2,5 diphenyl tetrazolium bromide; Na<sub>2</sub>PO<sub>4</sub>, disodium phosphate; NaHPO<sub>3</sub>, sodium hydrogen phosphate; OD, optical density; SCC, squamous cell carcinoma.

Amphotericin B) (Thermo Fisher Scientific, Waltham, MA) in a 37 °C incubator supplemented with 5% carbon dioxide.

### Lactate dimer synthesis

The synthesis of dimeric D-lactic acid was previously described in United States patent (US10034895B2) and was accomplished in five steps. The synthesis began with tert-butyl-diphenylsilyl protection of commercial D-(+)-methyl lactate. The ester was hydrolyzed to furnish the silyl-protected D-lactic acid, which was then coupled to benzyl (S)-(-)-lactate through Mitsunobu alkylation. The silyl group was removed in the presence of acetic acid/tetra-*n*-butylammonium fluoride. Catalytic hydrogenolysis of the benzyl group gave the

D-lactic acid dimer. The composition and purity of each intermediate as well as the final dimer were determined by liquid chromatography–mass spectrometry (electrospray ionization) and high field 1H/13C nuclear magnetic resonance spectroscopy.

### Cell growth and survival assay

For 3-(4,5-dimethylthiazol-2-yl)-2,5 diphenyl tetrazolium bromide assay, melanoma cells (A375 and A2058), SCC cells (A431, CAL27, and Fadu), and primary human dermal fibroblasts were seeded at  $8 \times 10^3$  cells per well in a 96-well plate, and after 24 hours, cells were treated in triplicates with increasing concentrations of DLAD or LLAD for 24, 48, and 72 hours. Cells were then incubated with 5

$\mu$ l 3-(4,5-dimethylthiazol-2-yl)-2,5 diphenyl tetrazolium bromide (20 mg/ml, Sigma-Aldrich, St Louis, MO) for 2 hours, and media were then replaced with DMSO. Absorbance was measured at 595 nm using a plate reader (Synergy H1, BioTek Instruments, Winooski, VT).

For MitoTracker red CMXRos staining, A375 cells were treated with increasing concentrations of DLAD (2.5, 5, 10 mg/ml) for 24 hours and then incubated with CMXRos fluorescent dye (Thermo Fisher Scientific). Images were taken using an Olympus BX41 fluorescent microscope (Olympus, Tokyo, Japan). For live/dead cell staining, A375 cells were seeded in a 35-mm cultures dish. The next day, cells were treated with increasing concentrations of DLAD (2.5, 5, 10 mg/ml) for 24 hours and then incubated with calcein-AM and ethidium homodimer-1 (Thermo Fisher Scientific) for 30 minutes for detection of live and dead cells, respectively. Staining was visualized using an Olympus BX41 fluorescent microscope.

### Animal studies

Animal studies were performed in compliance with Duke Animal Care and Use Committee. Nude immunodeficient mice were obtained from the Duke Cancer Center Isolation Facility (Durham, NC). Subcutaneous tumors were generated by injection of A2058 and A375 human melanoma cells (20,000 cells in 100  $\mu$ l PBS-to-matrigel [3:1]) (BD Bioscience, Franklin Lakes, NJ) on both flanks of the nude mice. When the tumors became palpable, intratumor injections of PBS, DLAD, and LLAD were administered at 5–10% tumor volume to reach 25–50 mg/ml ( $n = 6–10$  per group) every other day for up to 3 weeks. Tissue samples were collected at the end-point and embedded in optimal cutting temperature compound for cryosectioning.

### Protein analysis by immunostaining

For immunofluorescent staining, 5–6  $\mu$ m thick cryosections were fixed in cold 100% methanol for about 20 minutes, blocked with 10% horse serum, incubated with primary antibodies against Ki-67 (MA5-14520, Thermo Fisher Scientific), CD45 (Sc-53665, Santa Cruz Biotechnology, Dallas, TX), and F4/80 (123103, BioLegend, San Diego, CA), followed by detection with Florescent Dylight-555–conjugated secondary antibodies and counterstained with DAPI (Thermo Fisher Scientific). Images were taken with the Olympus BX41 fluorescent microscope.

### Statistical analysis

Cell growth data presented in the figures were obtained from at least three independent experiments and presented as the mean  $\pm$  SD. Tumor growth analyses were performed in two separate experiments with 6–10 subcutaneous tumors per group. The statistical difference in means between groups was evaluated in R Foundation for Statistical Computing (R Foundation, Vienna, Austria) using a two-tailed Student's *t*-test unless specified otherwise, and  $P < 0.05$  was considered statistically significant.

### Data availability statement

No large datasets were generated in this study.

### ORCIDiDs

Anushka Dikshit: <http://orcid.org/0000-0002-1681-7205>  
 Junqi Lu: <http://orcid.org/0000-0002-8972-9564>  
 Amy E. Ford: <http://orcid.org/0000-0002-1394-0128>  
 Simone Degan: <http://orcid.org/0000-0001-5417-1196>  
 Yingai J. Jin: <http://orcid.org/0000-0002-1263-1649>  
 Huiying Sun: <http://orcid.org/0000-0003-1162-5228>  
 Amanda Nicholas: <http://orcid.org/0000-0003-2657-2982>  
 April K.S. Salama: <http://orcid.org/0000-0002-8105-5374>

Georgia Beasley: <http://orcid.org/0000-0001-6387-9030>  
 David Gooden: <http://orcid.org/0000-0002-1447-7235>  
 Jennifer Y. Zhang: <http://orcid.org/0000-0002-4485-1750>

### AUTHOR CONTRIBUTIONS

Conceptualization: JYZ, AD, JL; Formal Analysis: AD, JL, AEF; Funding Acquisition: JYZ; Investigation: AD, JL, AEF, SD, YJJ, HS, DG; Project Administration: JYZ; Visualization: AD, JL, SD, AEF, YJJ; Writing - Original Draft Preparation: JYZ; Writing - Review and Editing: AD, JL, SD, AEF, AKSS, GB, DG, JYZ

### CONFLICT OF INTEREST

AKSS declares receiving research funding (paid to institution) from Bristol Myers Squibb, Merck, Immunocore, and Nektar Therapeutics and being on consulting/scientific advisory board for Iovance Biotherapeutics, Regeneron Pharmaceuticals, Novartis, and Pfizer. The remaining authors state no conflict of interest.

### ACKNOWLEDGMENTS

This work was supported by Friends in honor of Captain Christopher Allen and Department of Dermatology of Duke School of Medicine.

### REFERENCES

- Adeva M, González-Lucán M, Seco M, Donapetry C. Enzymes involved in l-lactate metabolism in humans. *Mitochondrion* 2013;13:615–29.
- Bai X, Flaherty KT. Targeted and immunotherapies in BRAF mutant melanoma: where we stand and what to expect [e-pub ahead of print]. *Br J Dermatol* 2020. <https://doi.org/10.1111/bjd.19394> (accessed August 11, 2021).
- Böhme I, Bosserhoff A. Extracellular acidosis triggers a senescence-like phenotype in human melanoma cells. *Pigment Cell Melanoma Res* 2020;33:41–51.
- Brand A, Singer K, Koehl GE, Kolitzus M, Schoenhammer G, Thiel A, et al. LDHA-associated lactic acid production blunts tumor immunosurveillance by T and NK cells. *Cell Metab* 2016;24:657–71.
- Chren MM, Linos E, Torres JS, Stuart SE, Parvataneni R, Boscardin WJ. Tumor recurrence 5 years after treatment of cutaneous basal cell carcinoma and squamous cell carcinoma. *J Invest Dermatol* 2013;133:1188–96.
- Colegio OR, Chu NQ, Szabo AL, Chu T, Rhebergen AM, Jairam V, et al. Functional polarization of tumour-associated macrophages by tumour-derived lactic acid. *Nature* 2014;513:559–63.
- Cullen JK, Simmons JL, Parsons PG, Boyle GM. Topical treatments for skin cancer. *Adv Drug Deliv Rev* 2020;153:54–64.
- de la Cruz-López KG, Castro-Muñoz LJ, Reyes-Hernández DO, García-Carrancá A, Manzo-Merino J. Lactate in the regulation of tumor microenvironment and therapeutic approaches. *Front Oncol* 2019;9:1143.
- Feng J, Yang H, Zhang Y, Wei H, Zhu Z, Zhu B, et al. Tumor cell-derived lactate induces TAZ-dependent upregulation of PD-L1 through GPR81 in human lung cancer cells. *Oncogene* 2017;36:5829–39.
- Fischer K, Hoffmann P, Voelkl S, Meidenbauer N, Ammer J, Edinger M, et al. Inhibitory effect of tumor cell-derived lactic acid on human T cells. *Blood* 2007;109:3812–9.
- García-Cañaveras JC, Chen L, Rabinowitz JD. The tumor metabolic microenvironment: lessons from lactate. *Cancer Res* 2019;79:3155–62.
- Goldberg JS. Stereocomplexes formed from select oligomers of polymer d-lactic acid (PDLA) and l-lactate may inhibit growth of cancer cells and help diagnose aggressive cancers-applications of the Warburg effect [published correction appears in *Perspect Medicin Chem* 2014;6:9]. *Perspect Medicin Chem* 2011;5:1–10.
- Goldberg JS, Weinberg JB. Local application of D-lactic acid dimer is selectively cytotoxic when applied to cancer cells. <https://dukespace.lib.duke.edu/cspace/bitstream/handle/10161/16493/US%20201800885394%20A1.pdf?sequence=2&isAllowed=y>; 2018. (accessed August 11, 2021).
- Gopalakrishnan V, Spencer CN, Nezi L, Reuben A, Andrews MC, Karpinets TV, et al. Gut microbiome modulates response to anti-PD-1 immunotherapy in melanoma patients. *Science* 2018;359:97–103.
- Guy GP Jr, Machlin SR, Ekwueme DU, Yabroff KR. Prevalence and costs of skin cancer treatment in the U.S., 2002–2006 and 2007–2011. *Am J Prev Med* 2015a;48:183–7.
- Guy GP Jr, Thomas CC, Thompson T, Watson M, Massetti GM, Richardson LC, et al. Vital signs: melanoma incidence and mortality trends and projections - United States, 1982–2030. *MMWR Morb Mortal Wkly Rep* 2015b;64:591–6.

- Houles T, Gravel SP, Lavoie G, Shin S, Savall M, Méant A, et al. RSK regulates PFK-2 activity to promote metabolic rewiring in melanoma. *Cancer Res* 2018;78:2191–204.
- Liu MH, Beynet DP, Gharavi NM. Overview of deep dermal fillers. *Facial Plast Surg* 2019;35:224–9.
- Lu J, Tan M, Cai Q. The Warburg effect in tumor progression: mitochondrial oxidative metabolism as an anti-metastasis mechanism. *Cancer Lett* 2015;356:156–64.
- Matson V, Fessler J, Bao R, Chongsuwat T, Zha Y, Alegre ML, et al. The commensal microbiome is associated with anti-PD-1 efficacy in metastatic melanoma patients. *Science* 2018;359:104–8.
- Mayeur C, Gratadoux JJ, Bridonneau C, Chegdani F, Larroque B, Kapel N, et al. Faecal D/L lactate ratio is a metabolic signature of microbiota imbalance in patients with short bowel syndrome. *PLoS One* 2013;8:e54335.
- Migden MR, Rischin D, Schmults CD, Guminski A, Hauschild A, Lewis KD, et al. PD-1 blockade with cemiplimab in advanced cutaneous squamous-cell carcinoma. *N Engl J Med* 2018;379:341–51.
- Persi E, Duran-Frigola M, Damaghi M, Roush WR, Aloy P, Cleveland JL, et al. Systems analysis of intracellular pH vulnerabilities for cancer therapy. *Nat Commun* 2018;9:2997.
- Ratnikov BI, Scott DA, Osterman AL, Smith JW, Ronai ZA. Metabolic rewiring in melanoma. *Oncogene* 2017;36:147–57.
- Rogers HW, Weinstock MA, Feldman SR, Coldiron BM. Incidence estimate of nonmelanoma skin cancer (keratinocyte carcinomas) in the U.S. population, 2012. *JAMA Dermatol* 2015;151:1081–6.
- Ruan GX, Kazlauskas A. Lactate engages receptor tyrosine kinases Axl, Tie2, and vascular endothelial growth factor receptor 2 to activate phosphoinositide 3-kinase/Akt and promote angiogenesis. *J Biol Chem* 2013;288:21161–72.
- San-Millán I, Brooks GA. Reexamining cancer metabolism: lactate production for carcinogenesis could be the purpose and explanation of the Warburg effect. *Carcinogenesis* 2017;38:119–33.
- Sun W, Liu Y, Glazer CA, Shao C, Bhan S, Demokan S, et al. TKTL1 is activated by promoter hypomethylation and contributes to head and neck squamous cell carcinoma carcinogenesis through increased aerobic glycolysis and HIF1alpha stabilization. *Clin Cancer Res* 2010;16:857–66.
- Tang T, Tang JY, Li D, Reich M, Callahan CA, Fu L, et al. Targeting superficial or nodular basal cell carcinoma with topically formulated small molecule inhibitor of smoothened. *Clin Cancer Res* 2011;17:3378–87.
- Tannock IF, Rotin D. Acid pH in tumors and its potential for therapeutic exploitation. *Cancer Res* 1989;49:4373–84.
- Webb BA, Chimenti M, Jacobson MP, Barber DL. Dysregulated pH: a perfect storm for cancer progression. *Nat Rev Cancer* 2011;11:671–7.



**This work is licensed under a Creative Commons Attribution-NonCommercial-NoDerivatives 4.0 International License. To view a copy of this license, visit <http://creativecommons.org/licenses/by-nc-nd/4.0/>**